Stereocomplex poly(lactic acid) nanocoated chitosan microparticles for the sustained release of hydrophilic drugs

Laura Pastorino[1*], Elena Dellacasa[1], Paola Petrini[2], Orietta Monticelli[3]

[1]Department of Informatics, Bioengineering, Robotics and Systems Engineering, University of Genoa, Genoa, Italy

[2]Department of Chemistry and Industrial Chemistry, University of Genoa, Genoa, Italy

[3]Department of Chemistry, Material and Chemical Engineering "G. Natta", Politecnico di Milano, Milan, Italy.

*laura.pastorino@unige.it

DOI: 10.1016/j.msec.2017.03.170

Abstract

In this work, novel chitosan based microparticles were developed by the layer-by-layer deposition of poly(lactic acid) stereocomplex films on their surface in the view of controlling the release of encapsulated hydrophilic drugs. As first step, the quartz crystal microbalance technique was used to monitor the step-by-step deposition of the stereocomplex layers onto chitosan by evaluating the deposited mass for each layer. Chitosan microparticles, with a size ranging between 40 and 90 μm, were then produced by an aerodynamically-assisted jetting technique and covered by a poly(lactic acid) stereocomplex shell. Infrared spectroscopy, wide X-ray diffraction, field emission scanning electron microscopy and contact angle measurements were used to verify the effective poly(lactic acid) adsorption onto chitosan microparticles and the stereocomplex formation. Finally, the release of a hydrophilic local anesthetic, procaine hydrochloride, from uncoated and stereocomplex-nanocoated microparticles was preliminary evaluated over a period of 15 days.

Keywords: chitosan; poly(lactic acid) stereocomplex; composite microparticles; sustained drug release; procaine hydrochloride

1. Introduction

Hydrogels can be formed both from synthetic and natural polymers, and they can be declined from bulk materials to particles, and from solid-like materials to injectable gels or coatings [1-4]. Drug molecules can be entrapped into the 3D hydrogel network to be released in vivo at a rate depending on the chemical-physical interaction of the drug with the macromolecular chain, the molecular mesh size, the surface/area ratio, and the nature of the surface of the hydrogel [4,5].

Chitosan (CHI), a copolymer of glucosamine and N-acetyl glucosamine, is a linear polysaccharide obtained by the deacetylation of chitin, the second most abundant natural

biopolymer derived from the exoskeleton of crustaceans and insects, which can behave as a polycation according to the pH of the medium [6]. CHI exhibits muco- and bio-adhesivity and its chemical functionality, reactive amino groups, may be exploited for further modification or induce electrostatic interactions with oppositely charged molecules [4,7]. For these reasons, CHI has great potential in biomedical applications, including tissue engineering, wound healing, drug and gene delivery [8-11].

However, the high-water content of hydrogels and, in some case, their fast degradation determines the fast release of water soluble encapsulated molecules [5]. To overcome such limitations, one strategy is based on the design of composite hydrogel systems with superior properties, besides mechanical and biological characteristics, in terms of degradation kinetics and/or tailored sustained release profiles [4,12-17].

In this respect, the modification of the surface of CHI nano- and micro-particles has been proposed in the literature as a promising approach to modulate drug release profiles [18,19].

As an example, coatings based on sodium alginate onto oral and mucosal delivery systems, via electrostatic interactions, were effective in limiting initial burst release and in prolonging drug release from CHI microparticles up to two days, probably due to the formation of a densely crosslinked surficial layer [20-23].

In the view of further prolonging drug release, we propose the modification of CHI microparticles by coating their surface with a hydrophobic synthetic polymer, such as poly(lactic acid) stereocomplex films deposited by Layer-by-Layer (LbL) technique.

Poly(lactic acid) (PLA) is a biodegradable polyester approved by the U.S. Food and Drug Administration for various biomedical applications, such as for the fabrication of scaffolds for tissue engineering, membranes, degradable sutures, bio-resorbable medical implants and drug delivery systems [24-26]. Poly(L-lactic acid) (PLLA) and poly(D-lactic acid) (PDLA) mixtures in polar organic solvents form triclinic racemic crystals, called stereocomplex, in

which the left- and right- forms pack side by side via van der Waals interactions [27-30]. The appeal of the stereocomplex-type PLA resides in its superior properties/performances with respect to the two single polymers: the stereocomplex form has a melting temperature of about 50 °C higher than that of PLLA and PDLA homo-crystals, higher stability/lower solubility in good solvents for either mere PLLA or PDLA, as well as enhanced crystallization rate, mechanical properties and the resistance to hydrolysis [31,32]. The above property is particular important in the development of systems to be applied in the biomedical field. Concerning the exploitation of stereocomplex PLA as surface coating, Serizawa et al. [28] first proved the stereocomplex formation by depositing enantiomeric PLA on a quartz crystal microbalance (QCM). Later, Akagi et al. [33] used an inkjet printing technique to produce PLA stereocomplex by the LbL deposition of PLLA, PDLA, and model drugs, whose release was controlled by simply varying the number of deposition cycles. More recently, always in the field of drug carriers, multifunctional nanoparticles were developed characterized by Fe_3O_4 magnetite as inner core, silica coatings as protective layer, and an outer shell consisting of stereocomplex PLA via a facile LbL method with highly tunable features [34]. Although stereocomplex PLA-based particles/micelles were widely exploited as delivery carriers themselves [35-38], the coating of biocompatible polymeric particles with stereocomplex was not investigated, despite the properties that such a deposition might confer to the system, especially in terms of drug release control.

Indeed, in our work, for the first time, the assembly of enantiomeric poly(lactide)s onto the surface of CHI microparticles was attempted, taking advantage of their cation-dipole interactions, as reported by Ogawa et al. for the assembly of PLA onto polylysine [39]. Ad hoc low molecular mass poly (L-lactic acid) (PLLA) and poly (D-lactic acid) (PDLA) were synthesized by ring-opening polymerization (ROP) of L- and D-lactides. As a first step, the quartz crystal microbalance technique was used to monitor the LbL assembly of PLA

stereocomplex onto quartz crystals modified with CHI and to evaluate the mass of the multilayers. CHI microparticles were then fabricated by an aerodynamically-assisted jetting technique. The obtained microparticles were modified by the LbL deposition of up to three (PDLA/PLLA) bilayers. Infrared spectroscopy, wide X-ray diffraction and contact angle analysis were used to verify the PLA effectively adsorption on the CHI microparticles and the stereocomplex formation. The morphology of plane and PLA modified CHI microparticles was characterized by scanning electron microscopy.

Furthermore, the developed system was characterized respect to its sustained release properties using as model hydrophylic drug procaine hydrochloride, a widely known local anesthetic [40-42].

2. Materials and Method

2.1. Materials

CHI (medium molecular weight, code 448877, lot MKBD4275V, from Pandalus Borealis), poly(ethyleneimine) (PEI, code 408727) and poly(styrenesulfonate) (PSS, code 243051), procaine hydrochloride (code P9879, water solubility 50 mg/ml), sodium hydroxide, acetic and sulfuric acid were purchased from Sigma-Aldrich. L-lactide (L-la) and D-lactide (D-la) (purity >98%) were kindly supplied by Purac Biochem. Before polymerization, both monomers were purified by three successive recrystallizions from 100% (w/v) solution in anhydrous toluene and dried under vacuum at room temperature. Ethylene glycol, a commercial product from Sigma-Aldrich (here simply referred to as ETG), was dried under vacuum at 40 °C for one night prior to use. Tin(II) 2-ethylhexanoate ($Sn(Oct)_2$, 95%) was purchased from Sigma-Aldrich and used without further treatments. All the solvents (*i.e.*, anhydrous toluene (≥99.7%), methanol and ethanol) were purchased from Sigma-Aldrich and used as received.

2.2. Methods

2.2.1. PLLA and PDLA synthesis

Poly (L-lactic acid) (PLLA) and poly (D-lactic acid) (PDLA) were synthesized by ring-opening polymerization (ROP) of L- and D-lactides, in bulk, employing $Sn(Oct)_2$ as a catalyst. In detail, about 10 g of L- or D-lactide were introduced and directly recrystallized into the reactor and there accurately dried (under vacuum at ambient temperature) and weighted under argon. A prescribed amount of the EG was added, under argon flow. The monomer to EG initiator molar ratio was calculated so as to obtain PLLA or PDLA having a number average molecular weight of 8000 g/mol. After the introduction of EG, the flask was evacuated for 15 minutes and purged with argon; these vacuum/argon cycles were repeated three times in order to thoroughly dry the reactants. The reaction vessel was then immersed into a thermostatically controlled oil bath set at 180 °C, while under stirring: as soon as the monomer and the initiator were molten and well mixed, about 1 ml of a freshly prepared solution of $Sn(Oct)_2$ in toluene ([lactide]/[$Sn(Oct)_2$] = 10^4) was added under argon, and the reaction allowed to proceed for 6 hours under inert atmosphere. After this time, the reaction mixture was cooled down by transferring the flask into an ice bath. The crude products were dissolved in chloroform, re-precipitated into an excess of n-hexane, filtered, and washed several times with cold methanol to remove the residual monomer. The polymers were dried in vacuum at 40 °C till constant weight, before characterization and employment.

The molecular mass, calculated by using ^{1}H-NMR, was found to be 8100 g/mol for both PLLA and PDLA and no racemization was found to occur. Moreover, GPC analysis gave a molecular weight distribution of 1.5 for both the above polymers.

2.2.2. Preparation of CHI microparticles

CHI was dissolved in 0.1 M acetic acid, to a final concentration of 1%w/v, by constant mechanical stirring at 1000 rpm for 2 hours. CHI microparticles were obtained by an

aerodynamically-assisted jetting equipment (Nisco Encapsulation Unit VAR J30) [43,44]. Briefly, the CHI solution was extruded through a conical nozzle, having a diameter of 0.25 mm, at a flow rate of 0.2 ml/min under 80 mbar pressure. The generated microdroplets were collected into a gelling solution bath (H_2O_{dd} 40%, Ethanol 60% and NaOH 2% w/v) [45] under continuous stirring. The microparticles were formed through a coacervation/precipitation process [46,47]. The distance from nozzle to the gelling solution was set at 6 cm. After allowing 30 min for the completion of solidification, the microparticles were thoroughly washed in distilled water by centrifugation (1000 rpm for 5 min) and used for the experiments.

2.2.3. Preparation of procaine loaded CHI microparticles

10 mg of lyophilized CHI microparticles were suspended in 15 ml of 50 mg/ml procaine solution in water for 48 h, under continuous shaking. Loaded microparticles were then moved from water to acetonitrile for the following enantiomeric poly(lactide)s adsorption. Three washings in acetonitrile were performed by centrifugation at 3000 rpm for 5 minutes, in order to eliminate all of the water. The collected supernatant was used to spectrophtometrically evaluate the amount of loaded drug. After that, 5 mg of loaded CHI microparticles were suspended in poly(lactide) acid solutions for their adsorption, whereas the remaining 5 mg were untreated, in order to compare drug release rates.

2.2.4. Quartz Crystal Microbalance

The assembly process onto planar supports was studied by the quartz crystal microbalance (QCM) technique. Gravimetric measurements were carried out by means of a home-made QCM using quartz crystals oscillators with resonance frequency of 10 MHz and with polished gold electrodes having a diameter of 14 mm. Before measurements, the gold electrodes of the quartz crystals were cleaned with H_2SO_4 at 150 °C for 30 min, followed by three washing steps in pure water and by a final drying step in nitrogen flux. The change in

resonance frequency was measured after each assembly step and correlated to the adsorbed polymer mass (Δm, ng) by the Sauerbrey

equation [48]:

$$-\Delta F(\mathrm{Hz}) = \frac{2F_0^2}{A\sqrt{\mu q \rho q}}\Delta m\ (\mathrm{ng}) \qquad (1)$$

where F_0 is the resonance frequency of the quartz crystal oscillator, A is the area of the gold electrode (0.205 cm^2), ρq is the quartz density (2.648 g/cm^3), and μq is its shear modulus ($2.947*10^{11}$ $g/cm\ s^2$). The following equations were derived from (1) and used in this work:

$$-\Delta F(\mathrm{Hz}) = 0.55\ \Delta m\ (\mathrm{ng}) \qquad (2)$$

The cleaned electrodes were immersed into the aqueous solutions of PSS and PEI (2 mg/ml) for 15 minutes and CHI (2 mg/ml in 0.1 M acetic acid) for 30 minutes, then taken out, rinsed thoroughly with pure water and dried with N_2. Since the quartz crystal surface is mostly negatively charged, PEI was deposited as the first layer. The (PEI/PSS) precursor bilayer was deposited in order to impart a negative charge, which is necessary for the subsequent electrostatic adsorption of CHI [49,50]. CHI was then adsorbed from a diluted solution (1mg/ml in 0.1M acetic acid) and then quartz crystal bearing a thin layer of CHI was put in contact with PLLA/PDLA solutions. These steps were carried out by immersing the crystal into acetonitrile solutions of PDLA and PLLA (10 mg/ml) for 20 min at 50 °C. Again, after removal from the PLA solutions, the coated electrodes were rinsed thoroughly with acetonitrile at 50 °C and dried with N_2. The deposition steps were repeated until the desired multilayered structure was obtained.

2.2.5. Assembly of the enantiomeric poly(lactide)s on the microparticle surfaces

The PLLA and PDLA deposition on the microparticle surface was done in a solvent of the polymers, namely acetonitrile (ACN). Indeed, in order to transfer the microparticles in ACN, 10 mL of the aqueous suspension, containing 9 mg of CHI, were centrifuged for 20 min at 1000 rpm, the surnatant solution was removed and 10 mL of ACN was added. This operation

was repeated for three times. The assembly of the enantiomeric poly(lactide)s was accomplished by contacting the microparticles alternatively with solutions of PLLA and PDLA in ACN. In detail: each layer was deposited eliminating the previous solution by centrifugation at 1000 rpm for 5 min and adding 10 mL of the polymer solution at a concentration of 10 mg/mL. The suspension was kept at 50 °C for 30 min under slow stirring. After this, the microparticles were washed by eliminating the solution through centrifugation and adding fresh solvent. This operation was repeated for six times.

2.3. Characterization of microparticles

To study the microparticle surface morphology, a Leica Stereoscan 440 scanning electron microscope was used. Prior to examination, all samples were freeze-dried and the surface was coated with carbon using a Polaron E5100 sputter coater. The microparticle diameters and their distribution were analyzed by coupling ImageJ 1.41 software-assisted image analysis and analytical measurement by Matlab software. Briefly, optical microscope images (inverted IX-51 Olympus microscope equipped with a DP70 digital camera and with a CPlan 103 objective) were converted to binary images, and the threshold of the binary was adjusted so that the particles to be measured were highlighted. Particles that were touching and separated by watershed segmentation. The processed images were measured using the analyze particles tool in the software, which generated a table outlining the particle areas. The data were then analyzed by Matlab, and the diameters were calculated and graphed.

Static wide-angle X-ray diffraction was carried out in reflection mode a Philips PW 1830 powder diffractometer (Ni-filtered Cu Ka radiation, k = 0.1542 nm).

FTIR spectra were recorded on a Bruker IFS66 spectrometer in the range 400-4000 cm^{-1}.

Contact angle measurements were performed at room temperature with an Erma G-1 contact angle meter using pure distilled water as probe liquid. The average static water contact angles were obtained by measuring at least three droplets on each specimen.

2.4. Preliminary procaine hydrochloride release characterization

Procaine release was performed in sterile water, at 37 °C and characterized at 291 nm by a UV-vis spectrophotometer (6705, Jenway, Bibby Scientific, UK) [51-53]. To this aim, as a first step the absorption spectra of procaine at different concentrations, (0,0025; 0,003125; 0,00375; 0,005; 0,00625; 0,0075; 0,01; 0,0125; 0,015; 0,02; 0,025; 0,03; 0,04; 0,05 mg/ml), were recorded and the calibration curve was thus established (y=74,522x-0,0169, where y is the absorbance and x procaine concentration, with a correlation coefficient R^2 = 0,99472).

Both specimen, uncoated CHI and enantiomeric PLAs coated loaded microparticles, were placed in 40 µm cell strainer and then in 6 ml well plates. At each collection time (15 min, 30 min, 1 h, 4 h, 24 h, 48 h, 360 h), 1 ml of water containing the released procaine was replaced by 1ml of fresh sterile water. The procaine content in the aliquots was measured at room and the concentration was calculated using the calibration curve, taking into account the dilution factor at each withdrawal point. The test was performed in triplicate and the results were expressed as mean ± standard deviation.

3. Results and discussion

The LbL assembly of CHI and PLAs was characterized by the QCM technique by monitoring the effective step-by-step multilayer growth (Figure 1). The QCM frequency shift, due to the deposition of material onto the electrode surface, was measured and the related adsorbed mass was calculated [54,55]. The CHI/$(PDLA/PLLA)_3$ multilayer was deposited on the crystal surface, previously functionalized by the deposition of a (PEI/PSS) precursor bilayer.

Since the quartz crystal surface is weakly negatively charged, the (PEI/PSS) precursor was deposited as the first bilayer, in order to promote the adsorption of the positive CHI layer [49,50]. The (PEI/PSS)/CHI multilayer structure showed a total mass of 621±96 ng, where the CHI was found to have a mean adsorbed mass of 158±53 ng (as the result of the mean of

three samples). The total mass of adsorbed PLA layers was found to be 501±69 ng. The gradual growth of the PLA layers confirmed the successful deposition of the polymers [29].

In addition, the adsorbed mass of PLA layers seems to increase with the deposition steps.

The higher mass deposition can be driven by the formation of the stereocomplex between PDLA and PLLA polymers; according to literature [28,29], the formed "dotted" structure that could increase the available surface area for deposition at each step. The slight increase in mass for the first layers could be due to a non-uniform deposition related to the exchange of deposition conditions [56].

The CHI microparticles were obtained by generating CHI microdroplets, using the bead generator, and by phase inversion (liquid to solid) in NaOH, exploiting the decrease of solubility of chitosan at acidic to basic pH. The optimization of the instrumental parameters, namely chitosan flow rate and pressure at the exit of the nozzle, leaded to microparticles with narrow diameter distribution and without any aggregation.

Results indicated a spherical shape and a size ranging from 40 to 90 µm, with an average dimeter of 66 ± 10 µm. This result was also confirmed by the FE-SEM characterization.

In order to verify the chemical composition of the coated microparticles and to detect eventual interaction of chitosan and PLA, FT-IR measurements were carried out. Figure 3 compares IR spectra of PLLA (PDLA) with that of the uncoated and coated microparticles.

The spectra of the coated and uncoated microparticles were found to be similar, as the main peaks at 3450 cm^{-1}, 1647 cm^{-1}, 1570 cm^{-1}, 1150 cm^{-1} and 890 cm^{-1}, that is the typical absorption bands of CHI [57]. Nevertheless, in the coated microparticles spectrum (Fig. 3c) additional peaks were detected at 1750 cm^{-1} and at 1192 cm^{-1}, which can be assigned to the carbonyl bond of the ester group of the PLLA and the C-O stretching mode of the ester respectively. These findings corroborated the presence of a PLA layer onto the surface of the CHI microparticles. Although ATR FTIR is considered a surface analysis, as the penetration

depth of the IR is in the order of few micrometers, the spectral contribution of CHI is clearly detectable, and the spectrum reports the average composition of the nanometric coating plus the CHI core. The spectrum of the assembled system was found to be approximated to the sum of the individual spectra of the two substances, CHI and PLA, with no changes in the spectral pattern appearing, supporting the hypothesis that no reaction occurs between CHI and PLA. Previous studies on chitosan/polylactic acid blends have also shown that no specific interaction between the two polymers is established, other than hydrogen bonds between amino (in chitosan) and carboxyl groups (in PLA) [58]. Moreover, Ogawa et al. [39] reported the deposition of films composed of PLA and polylysine through cation−dipole interaction.

The morphology of the freeze-dried CHI microparticles, both before and after the LbL assembly of the $(PLLA/PDLA)_3$ multilayer, was characterized by SEM. Figure 4 shows FE-SEM images of uncoated microparticles. In particular, the fragment of internal structure of the uncoated microparticles, shown in Figure 4, was characterized by high porosity, with pores of greater size than those observed on the surface.

The images in Figure 5 show that the morphology of the surface of uncoated CHI microparticles was rough and highly porous (Figure 5 left), whereas the morphology of the coated ones seemed to be smoother and grainy (Figure 5 center and right). The observed differences could be due to presence of the polymeric coating.

To evaluate the influence of the PLA coating on the surface wettability, contact angle measurements were carried out. Indeed, these measurements are considered to be important to assess the surface properties of the solid surface, governed by both the surface chemical composition and by its geometrical microstructure.

The contact angle of the microspheres, before and after the coating, was found to be significantly different. In particular, while the surface of the uncoated microparticles was

found to be characterized by a contact angle of 88° ± 12°, a value similar to that reported in the literature for the neat CHI film [59], the contact angle of the coated microparticles turned out to be much higher, it being 150° ± 6°. The latter value is significantly different with respect to the contact angle which is reported for the neat PLA film, that is 73° [60]. By combining this information with our results, it is possible to hypothesize that the hydrophobic properties of the coated microparticles are not due to the chemical nature of the outer coating, which is made of PLA, but rather to the increase of the surface roughness, as evidenced by FE-SEM measurements.

The coated particles were analyzed by means of WAXD, as this is considered one of the most effective method for monitoring PLA stereocomplexation. In the WAXD pattern of the coated microparticles, reported in Figure 6, intense peaks are observed at 2θ values of 12°, 21°, and 24°. The spectra of PDLA and PLLA are characterized by peaks at 15°, 17 [26], so that the observed peaks were attributed to PLA stereocomplex crystals with a triclinic unit cell of dimensions a=0.916 nm, b=0.916nm, c=0.870 nm, α=109.2, β=109.2 and γ=109.2, where L-lactide and D-lactide segments are packed laterally in parallel fashion by taking 3l helical conformation [26]. This finding demonstrates the effectiveness of the approach used to deposit the PLLA-PDLA layers onto the surface of CHI microparticle in promoting the structuring of the polymer.

Finally, procaine was loaded in the CHI microparticles for release behavior characterization. In a first attempt procaine was dissolved in the CHI solution and then microparticles were formed. However, since procaine is water and ethanol soluble, procaine was almost totally lost during the neutralization process, so that a post loading protocol on lyophilized microparticles was adopted [61,62]. Figure 7 (left) shows the absorption spectra for procaine hydrochloride while figure 7 (right) shows the release behavior of procaine from uncoated

CHI microparticles and coated ones at various collection times (15 min, 30 min, 1 h, 4 h, 24 h, 48 h, 96 h and 360h) measured by Uv-vis spectroscopy.

The release profile of procaine form coated CHI microparticles decreased. The procaine release from uncoated CHI microparticles was characterized by an initial burst release, resulting in the release of almost 90% of the loaded drug within the first 15 minutes. In this case, the release was completed after 96 hours. Compared with the uncoated microparticles, procaine release from stereocomplex-coated microparticles decreased, showing a reduction in the burst phenomenon. Around 30% of encapsulated drug was released in the first 96 h, reaching the 34% after 360 h. These results reveal that the presence of the stereocomplex multilayer, decreasing the porosity of the developed system, acts as a barrier for the procaine diffusion.

These results are responding to a major challenge in local anesthetic release: an overdose of these drugs results in severe systemic toxicity. Many different systems are recently studied to avoid burst release [63-67] witnessing the clinical need of new systems for pain management in postoperative surgery [68].

4. Conclusions

In this study, composite microparticles based on the LbL deposition of PLA stereocomplex films onto the surface of CHI microparticles were developed, optimized and tested for the sustained release of procaine hydrochloride. The composite delivery system was fully characterized and the results confirmed the successful modification of the microparticles and the formation of the stereocomplex layers. The effect of the superficial modification on the release behavior of the model drug procaine revealed that the burst phenomenon was limited, that the release was slowed and not completed after 15 days of monitoring. These results represent a starting point for future studies aimed at developing anesthetic release systems.

Acknowledgements

This work was partially supported by Fondazione Banca del Monte di Lombardia to P.Petrini.

References

1. T.R. Hoare, D.S. Kohane, Hydrogels in drug delivery: progress and challenges, Polymer 49(8) (2008) 1993-2007.
2. F. Munarin, P. Petrini, S. Bozzini, M.C. Tanzi, New perspectives in cell delivery systems for tissue regeneration: Natural-derived injectable hydrogels, Journal of Applied Biomaterials and Functional Materials 10 (2) (2012) 67-81.
3. T. Coviello, P. Matricardi, C. Marianecci, F. Alhaique, Polysaccharide hydrogels for modified release formulations, Journal of Controlled Release 119(1) (2007) 5-24.
4. M. Rinaudo, Chitin and chitosan: properties and applications, Progress in Polymer Science 31(7) (2006) 603-632.
5. T. Kean, M. Thanou, Biodegradation, biodistribution and toxicity of chitosan, Advanced Drug Delivery Reviews 62(1) (2010) 3-11.
6. A.Anitha, S. Sowmya, P.T. Sudheesh Kumar, S. Deepthi, K.P. Chennazhi, H. Ehrlich, M. Tsurkan, R. Jayakumar, Chitin and chitosan in selected biomedical applications, Progress in Polymer Science 39 (2014) 1644-1667.
7. V.K. Mourya, N.N. Inamdar, Chitosan-modifications and applications: opportunities galore, React. Funct. Polym. 68 (2008) 1013–1051.
8. J.K.F. Suh, H.W.T. Matthew, Application of chitosan-based polysaccharide biomaterials in cartilage tissue engineering: a review, Biomaterials 21 (2000) 2589–2598.
9. R.A.A. Muzzarelli, Chitins and chitosans for the repair of wounded skin, nerve, cartilage and bone, Carbohydr. Polym. 76 (2009) 167–182.
10. M. Paini, B. Aliakbarian, A.A. Casazza, P. Perego, C. Ruggiero, L. Pastorino, Chitosan/dextran multilayer microcapsules for polyphenol co-delivery, Materials Science and Engineering: C 46 (2015) 374-380.

11. L. Pastorino, S. Erokhina, C. Ruggiero, V. Erokhin, P. Petrini, Fabrication and Characterization of Chitosan and Pectin Nanostructured Multilayers. Macromolecular Chemistry and Physics 216(10) (2015) 1067-1075.
12. S. Ladet, L. David, A. Domard, Multi-membrane hydrogels, Nature 452 (2008) 76–79.
13. T. Jiang, W.I. Abdel-Fattah, C.T. Laurenc, In vitro evaluation of chitosan/poly(lactic acid-glycolic acid) sintered microsphere scaffolds for bone tissue engineering, Biomaterials 27 (2006) 4894-4903.
14. T. Jiang, S.P. Nukavarapu, M. Deng, E. Jabbarzadeh, M.D. Kofron, S.B. Doty, W.I. Abdel-Fattah, C.T. Laurencin, Chitosan-poly(lactide-co-glycolide) microsphere-based scaffolds for bone tissue engineering: In vitro degradation and in vivo bone regeneration studies, Acta Biomaterialia 6 (2010) 3457-3470.
15. L. Li, S. Ding, C. Zhou, Preparation and degradation of PLA/chitosan composite materials, Journal of Applied Polymer Science 91 (2004) 274-277.
16. M. Tunesi, E. Prina, F. Munarin, S. Rodilossi, D. Albani, P. Petrini, C. Giordano, Cross-linked poly(acrylic acids) microgels and agarose as semi-interpenetrating networks for resveratrol release, Journal of Materials Science. Materials in medicine 26 (1) (2015) 1-11.
17. N. Kamaly, B. Yameen, J. Wu, O.C. Farokhzad, Degradable controlled-release polymers and polymeric nanoparticles: Mechanisms of controlling drug release, Chemical Reviews 116 (2016) 2602-2663.
18. M. George, T.E. Abraham, Polyionic hydrocolloids for the intestinal delivery of protein drugs: alginate and chitosan—a review, Journal of Controlled Release 114 (2006) 1-14.

19. V.R. Sinha, A.K. Singla, S. Wadhawan, R. Kaushik, R. Kumria, K. Bansal, S. Dhawan, Chitosan microspheres as a potential carrier for drugs, International Journal of Pharmaceutics 274 (2004) 1-33.
20. O. Borges, A. Cordeiro-da-Silva, S.G. Romeijn, M. Amidi, A. de Sousa, G. Borchard, H.E. Junginger, Uptake studies in rat Peyer's patches, cytotoxicity and release studies of alginate coated chitosan nanoparticles for mucosal vaccination. Journal of Controlled Release 114 (2006) 348-358.
21. A. Shukla, V. Mishra, B.S. Bhoop, O.P. Katare, Alginate coated chitosan microparticles mediated oral delivery of diphtheria toxoid.(Part A). Systematic optimization, development and characterization, International Journal of Pharmaceutics 495 (2015) 220-233.
22. A.P. Bagre, K. Jain, N.K. Jain, Alginate coated chitosan core shell nanoparticles for oral delivery of enoxaparin: in vitro and in vivo assessment, International Journal of Pharmaceutics 456 (2013) 31-40.
23. X. Li, X. Kong, S. Shi, X. Zheng, G. Guo, Y. Wei, Z. Qian, Preparation of alginate coated chitosan microparticles for vaccine delivery, BMC Biotechnology 8 (2008) 89.
24. R.E. Drumright, P.R. Gruber, D.E. Henton, Polylactic acid technology, Advanced Materials, 12 (2000) 1841-1846.
25. A.J. Lasprilla, G.A. Martinez, B.H. Lunelli, A.L. Jardini, R. Maciel Filho, Poly-lactic acid synthesis for application in biomedical devices—A review, Biotechnology Advances 30 (2012) 321-328.
26. H. Tsuji, Poly(lactide) stereocomplexes: formation, structure, properties, degradation, and applications, Macromol. Biosci. 5 (2005) 569–597.
27. K. Kondo, T. Kida, Y. Ogawa, Y. Arikawa, M. Akashi, Nanotube formation through the continuous one-dimensional fusion of hollow nanocapsules composed of layer-by-

layer poly (lactic acid) stereocomplex films, Journal of the American Chemical Society 132 (2010) 8236-8237.

28. T. Serizawa, H. Yamashita, T. Fujiwara, Y. Kimura, M. Akashi, Stepwise assembly of enantiomeric poly (lactide)s on surfaces, Macromolecules 34 (2001) 1996-2001.
29. E. Dellacasa, L. Zhao, G. Yang, L. Pastorino, G.B. Sukhorukov, Fabrication and characterization of novel multilayered structures by stereocomplexion of poly (D-lactic acid)/poly (L-lactic acid) and self-assembly of polyelectrolytes, Beilstein J. Nanotechnol. 7 (2016) 81–90.
30. M. Matsusaki, H. Ajiro, T. Kida, T. Serizawa, M. Akashi, Layer-by-Layer Assembly Through Weak Interactions and Their Biomedical Applications, Adv. Mater. 24 (2012) 454–474.
31. S.R. Andersson, M. Hakkarainen, S. Inkinen, A. Södergård, A.C. Albertsson, Customizing the hydrolytic degradation rate of stereocomplex PLA through different PDLA architectures, Biomacromolecules 13 (2012) 1212−1222.
32. O. Monticelli, M. Putti, L. Gardella, D. Cavallo, A. Basso, M. Prato, S. Nitti, New stereocomplex PLA-based fibers: Effect of POSS on polymer functionalization and properties, Macromolecules 47 (2014) 4718−4727.
33. T. Akagi, T. Fujiwara, M. Akashi, Inkjet printing of Layer-by-Layer assembled poly(lactide) stereocomplex with encapsulated proteins, Langmuir 30 (2014) 1669−1676.
34. Z. Li, D. Yuan, G. Jin, B. H. Tan, C. He, Facile Layer-by-Layer self-assembly toward enantiomeric poly(lactide) stereocomplex coated magnetite nanocarrier for highly tunable drug deliveries, ACS Appl. Mater. Interfaces 8 (2016) 1842−1853.
35. R. Slivniak, A. J. Domb, Stereocomplexes of enantiomeric lactic acid and sebacic Acid ester−anhydride triblock copolymers, Biomacromolecules 3 (2002) 754−760.

36. L. Chen, Z. Xie, J. Hu, X. Chen, X. Jing, Enantiomeric PLAPEG block copolymers and their stereocomplex micelles used as Rifampin delivery, J. Nanopart. Res. 9 (2007) 777−785.
37. F. Nederberg, E. Appel, J. P. K. Tan, S. H. Kim, K. Fukushima, J. Sly, R. D. Miller,R. M. Waymouth, Y. Y. Yang, J. L. Hedrick, Simple approach to stabilized micelles employing miktoarm terpolymers and stereocomplexes with application in paclitaxel delivery, Biomacromolecules, 10 (2009) 1460−1468.
38. Y. Zhu, T. Akagi, M. Akashi, Self-assembling stereocomplex nanoparticles by enantiomeric poly(γ-glutamic acid)-poly(lactide) graft copolymers as a protein delivery carrier, Macromol. Biosci. 14 (2014) 576−587.
39. Y. Ogawa, Y. Arikawa, T. Kida, M. Akashi, Fabrication of novel layer-by-layer assembly films composed of poly (lactic acid) and polylysine through cation− dipole interactions. Langmuir 24 (2008) 8606-8609.
40. J.P.K. Tan, A.Q.F. Zeng, C.C. Chang, K.C. Tam, Release kinetics of procaine hydrochloride (PrHy) from pH-responsive nanogels, Theory and Experiments, International Journal of Pharmaceutics 357 (2008) 305–313.
41. E. de Paula, C.M. Cereda, L.F. Fraceto, D.R. de Araujo, M. Franz-Montan, G.R. Tofoli, J. Ranali, M.C. Volpato, F.C. Groppo, Micro and nanosystems for delivering local anesthetics, Expert Opinion on Drug Delivery 9 (2012) 1505-1524.
42. T. Govender, S. Stolnik, M.C. Garnett, L. Illum, S.S. Davis, PLGA nanoparticles prepared by nanoprecipitation: drug loading and release studies of a water soluble drug, Journal of Controlled Release 57 (1999) 171-185.
43. C. A. Custódio, V.E. Santo, M.B. Oliveira, M.E. Gomes, R.L. Reis, J.F. Mano, Functionalized microparticles producing scaffolds in combination with cells, Advanced Functional Materials 24 (2014) 1391-1400.

44. C.A.Custódio, M.T. Cerqueira, A.P. Marques, R.L. Reis, J.F. Mano, Cell selective chitosan microparticles as injectable cell carriers for tissue regeneration, Biomaterials 43 (2015) 23-31.

45. Q. He, Q. Ao, Y. Gong, X. Zhang, Preparation of chitosan films using different neutralizing solutions to improve endothelial cell compatibility, Journal of Materials Science: Materials in Medicine 22 (2011) 2791-2802.

46. H.Q. Mao, K. Roy, V.L. Troung-Le, K.A. Janes, K.Y. Lin, Y. Wang, J.T. August, K.W. Leong, Chitosan-DNA nanoparticles as gene carriers: synthesis, characterization and transfection efficiency. Journal of Controlled Release 70 (2001) 399-421.

47. M. Dash, F. Chiellini, R.M, Ottenbrite, E. Chiellini, Chitosan—A versatile semi-synthetic polymer in biomedical applications, Progress in polymer science 36 (2011) 981-1014.

48. G.Z. Sauerbrey, Verwendung von schwingquartzen zur wagung dunner schichten und zur mikrowagung, Z Phys 155 (1959) 206–218.

49. Y. Lvov, K. Ariga, I. Ichinose, T. Kunitake, Assembly of multicomponent protein films by means of electrostatic layer-by-layer adsorption, J. Am. Chem. Soc. 117 (1995) 6117–6123.

50. L. Pastorino, S. Disawal, C. Nicolini, Y.L. Lvov, V.V. Erokhin, Complex catalytic colloids on the basis of firefly luciferase as optical nanosensor platform, Biotechnology and Bioengineering 84 (2003) 286-291.

51. L.M. Geever, C.C. Cooney, J.G. Lyons, J.E. Kennedy, M.J. Nugent, S. Devery, C.L. Higginbotham, Characterisation and controlled drug release from novel drug-loaded hydrogels, European Journal of Pharmaceutics and Biopharmaceutics 69 (2008) 1147-1159.

52. A. Lammel, M. Schwab, M. Hofer, G. Winter, T. Scheibel, Recombinant spider silk particles as drug delivery vehicles. Biomaterials 32 (2011) 2233-2240.

53. D. Ciolacu, C. Rudaz, M. Vasilescu, T. Budtova, Physically and chemically cross-linked cellulose cryogels: Structure, properties and application for controlled release. Carbohydrate Polymers 151 (2016) 392-400.

54. D.A. Buttry, M.D. Ward, Measurement of interfacial processes at electrode surfaces with the electrochemical quartz crystal microbalance, Chemical Reviews 92 (1992) 1355-1379.

55. K.A. Marx, Quartz crystal microbalance: a useful tool for studying thin polymer films and complex biomolecular systems at the solution-surface interface, Biomacromolecules 4 (2003) 1099-1120.

56. D.T. Haynie, S. Balkundi, N. Palath, K. Chakravarthula, K. Dave, Polypeptide multilayer films: role of molecular structure and charge, Langmuir 20 (2004) 4540-4547.

57. J. Brugnerotto, J. Lizardi , F. M. Goycoolea, W. Argüelles-Monal, J. Desbrièresa, M. Rinaudo. An infrared investigation in relation with chitin and chitosan characterization. Polymer 2011, 42, 3569-358.

58. Y. Wan, H. Wu, A. Yu, D. Wen, Biodegradable polylactide/chitosan blend membranes, Biomacromolecules 7 (2006) 1362-1372.

59. S. Rivero, M.A. García, A. Pinotti, Physical and chemical treatments on chitosan matrix to modify film properties and kinetics of biodegradation, Journal of Materials Physics and Chemistry 1 (2013) 51-57.

60. O. Monticelli, S. Bocchini, L. Gardella, D. Cavallo, P. Cebe, G. Germelli, Impact of synthetic talc on PLLA electrospun fibers, European Polymer Journal, 49 (2013) 2572-2583.

61. S.W. Kim, Y.H. Bae, T. Okano, Hydrogels: swelling, drug loading, and release. Pharmaceutical Research 9 (1992) 283-290.

62. N. Bhattarai, J. Gunn, M. Zhang, Chitosan-based hydrogels for controlled, localized drug delivery. Advanced Drug Delivery Reviews 62 (2010) 83-99.

63. D. Ciolacu, C. Rudaz, M. Vasilescu, T. Budtova, Physically and chemically cross-linked cellulose cryogels: Structure, properties and application for controlled release, Carbohydrate Polymers 151 (2016) 392-400.

64. L. Zorzetto, P. Brambilla, E. Marcello, N. Bloise, M. De Gregori, L. Cobianchi, A. Peloso, M. Allegri, L. Visai, P. Petrini, From micro- to nanostructured implantable device for local anesthetic delivery, Int. J. Nanomedicine 11 (2016)2695-709.

65. G. Petrisor, R.M. Ion, C.H. Brachais, J-P. Couvercelle, O. Chambin, Designing Medical Devices Based on Silicon Polymeric Material with Controlled Release of Local Anesthetics, Journal of Macromolecular Science, Part A: Pure and Applied Chemistry 49 (2012) 439-444.

66. C.F. Weiniger, L. Golovanevski, A.J. Domb, D. Ickowicz, Extended release formulations for local anaesthetic agents, Anaesthesia, 67 (2012) 906–916.

67. J.P Tan, Q. Wang, K.C. Tam, Control of burst release from nanogels via layer by layer assembly. Journal of Controlled Release, 128 (2008) 248-254.

68. P. Bhusal, J. Harrison, M. Sharma, D.S. Jones, A.G. Hill, D. Svirskis, Controlled release drug delivery systems to improve post-operative pharmacotherapy, Drug Delivery and Translational Research (2016) 1-11.

Figure legends

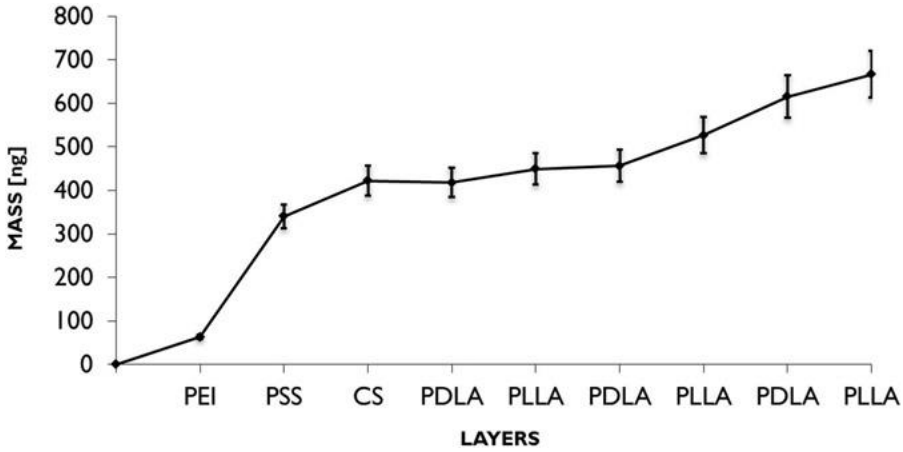

Figure 1: (PEI/PSS)/CHI/$(PDLA/PLLA)_3$ multilayer deposition on the crystal surface.

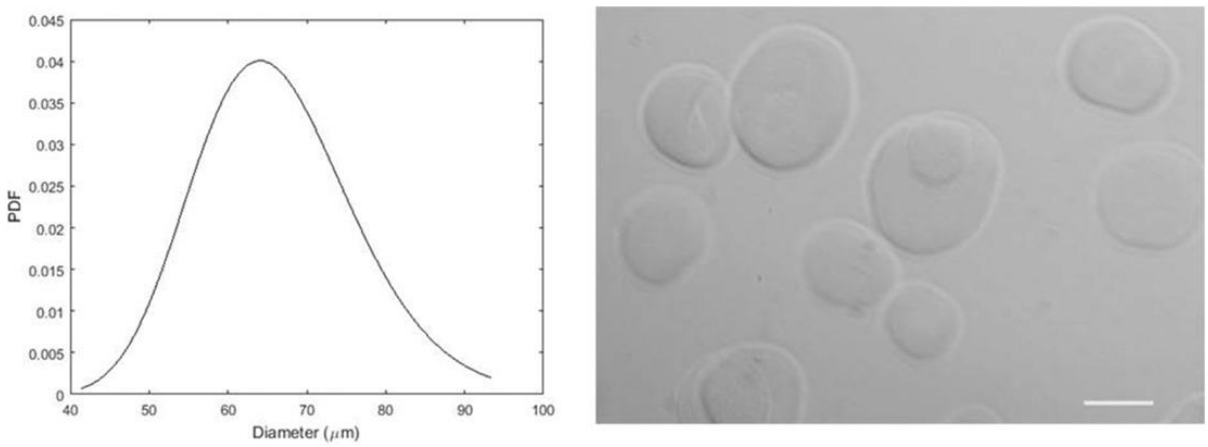

Figure 2: Probability Density Function of CHI microparticle diameters (left). Optical microscopy image of CHI microparticles. Scale bar: 50 μm (right).

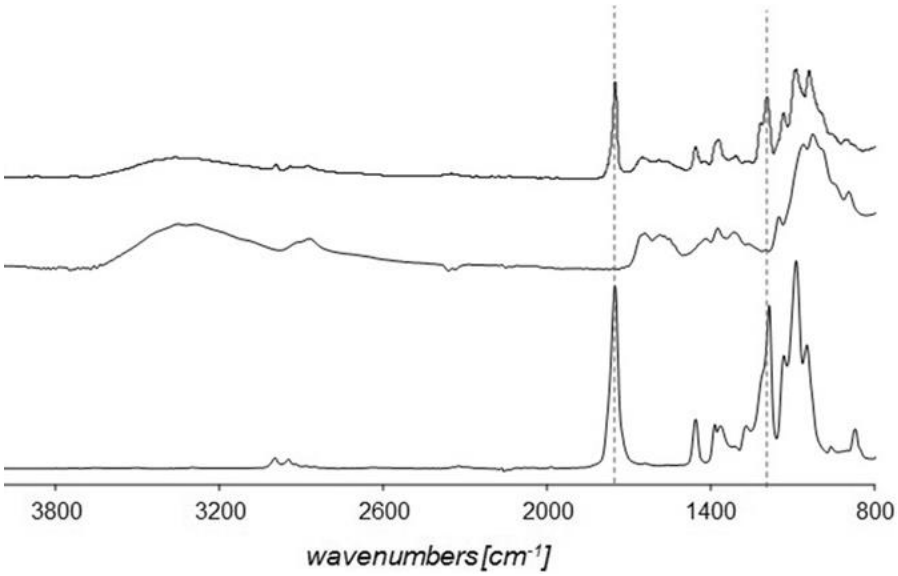

Figure 3: FT-IR spectra of: (a) PLLA (PDLA), (b) uncoated microparticles and (c) coated microparticles.

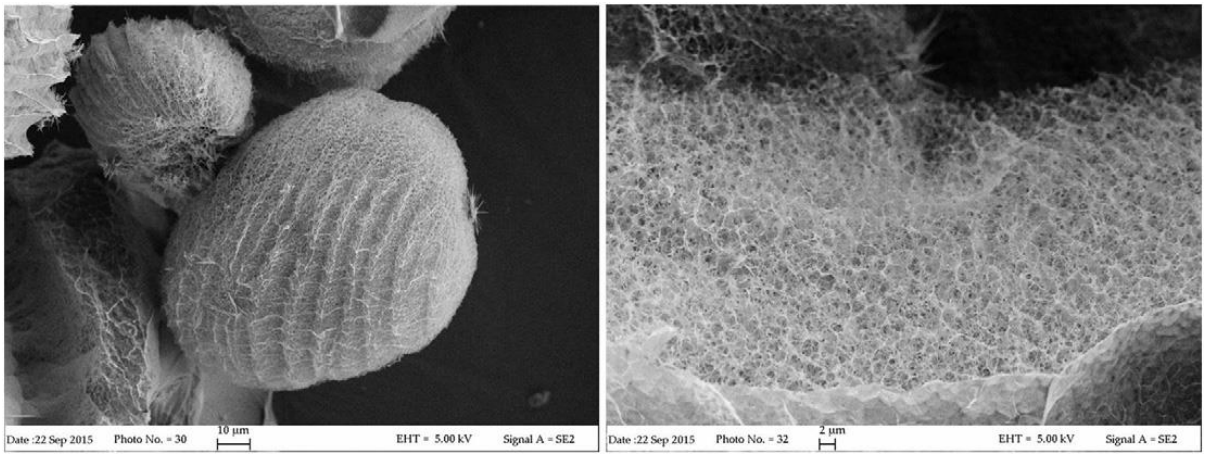

Figure 4: FE-SEM images of uncoated microparticles (left) and magnification of the microparticle internal structure (right).

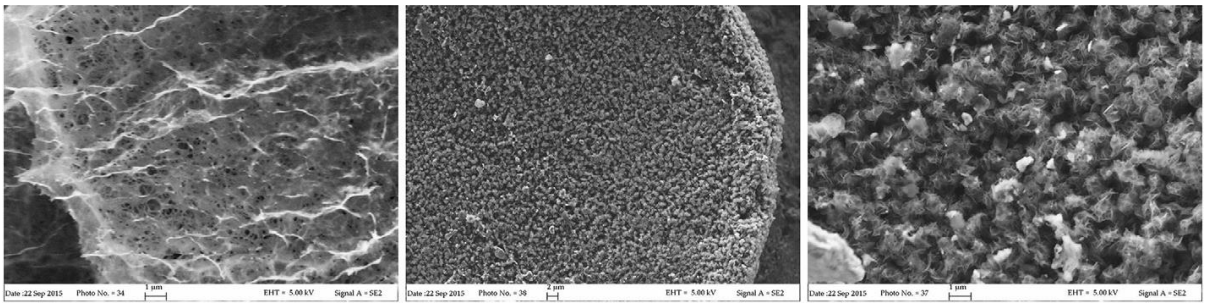

Figure 5: FE-SEM images of uncoated (left) and coated (center) microparticles, and magnification of coated microparticle shell (right)

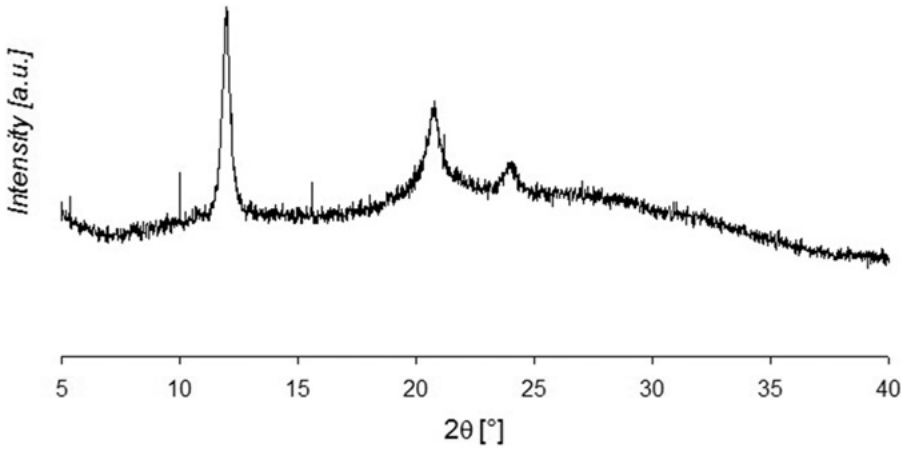

Figure 6. WAXD profile of the coated microparticles.

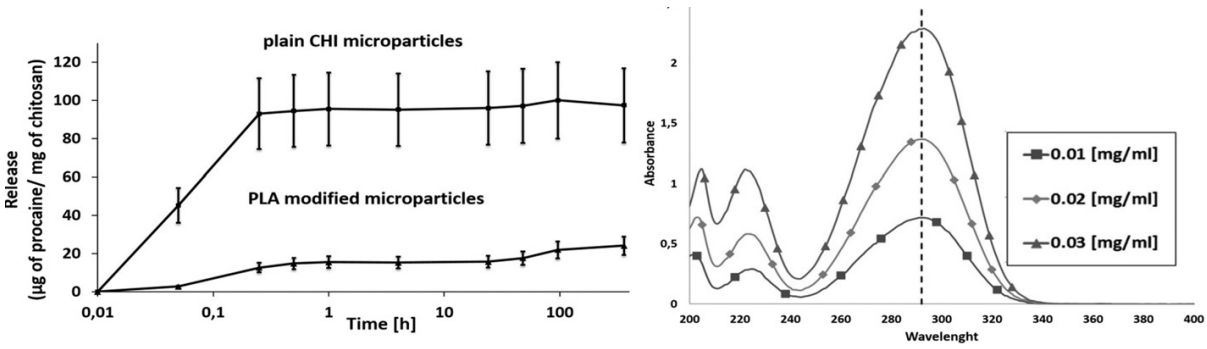

Figure 7. Release profile of procaine from coated and uncoated CHI microparticles (left) and absorption spectra for 0.01, 0.02, 0.03 mg/ml procaine hydrochloride in water (right).